



P-255

Clay anisotropy and gas hydrate saturation in KG Basin, eastern offshore India: Site 15

Ranjana Ghosh *, Kalachand Sain, and Maheswar Ojha

National Geophysical Research Institute (Council of Scientific and Industrial Research)

Summary

Clay-rich marine sediment of Krishna-Godavari (KG) basin in the eastern Indian margin has been described by the Indian National Gas-hydrate Program Expedition-1 as one of the richest hosts of gas-hydrate deposits in the world. Stable carbon isotope analyses indicate most of the gas-hydrate occurrences discovered during this expedition appear to contain predominantly methane which was generated by microbial processes. Resistivity at-bit images and pressure cores reveal that gas-hydrate occurs as either pore-filling grains or particles disseminated in coarser grain sediments or as a fracture-filling material in clay dominated sediments. Sites NGHP-01-3, 14, 15, 16, 17, 19, 20 of KG Basin are the places where gas-hydrate is found in sand layers/laminae within clay-rich sedimentary column. Clay-rich sediment has inherent anisotropy due to the orientation distribution pattern of clay platelets. The degree of anisotropy depends on the precise orientation distribution pattern of the clay platelets. Here, we have applied the effective medium theory (EMT) to determine the coefficient of orientation distribution function (ODF) of clay platelets and the amount of gas hydrate. The determined coefficients show the sediment is highly anisotropic. Using the anisotropy factor of clay platelets gas-hydrate is quantified from the well data of Site-15. Maximum gas hydrate is concentrated at ~ 80 meter below seafloor (mbsf) with an amount of ~50% of pore space.

Introduction

Gas-hydrates occur naturally at low temperature and high pressure conditions if supply of methane is sufficient. The mapping of gas-hydrates bearing sediments can be made by identifying BSR in the seismic sections or by direct evidences from drilling & coring. Marine sediments of the continental margins and the sediments of permafrost regions are found as suitable hosts for gas-hydrates. The amount of methane trapped within or below the hydrated layer is speculated to be double of all other fossil fuels. But accurate quantification of gas-hydrates is required to exploit gas economically. Gas-hydrates occupy the pore spaces of sand-rich sediments and sand layers in clay-rich sedimentary column or the cracks in the clay-rich sediments. Change of velocity with respect to the background is the most prominent property of gas-hydrates bearing sediment. There are several rock physics models to interpret the observed seismic velocity in terms of gas-hydrates and/or free gas saturation. The models based on the empirical relations, which assumes homogeneous and

isotropic sediments, are certainly not applicable in all geological conditions. Also clay-rich sediments have inbuilt anisotropy due to the orientation of spheroidal clay platelets and anisotropy generated due to the presence of fractures. After reviewing several theories, an effective medium theory (EMT), which is a combination of self-consistent approximation (SCA) and differential effective medium (DEM) theory coupled with smoothing approximation of crystalline aggregate, is selected for calculating the elastic properties with a view to assessing gas-hydrates from measured velocities.

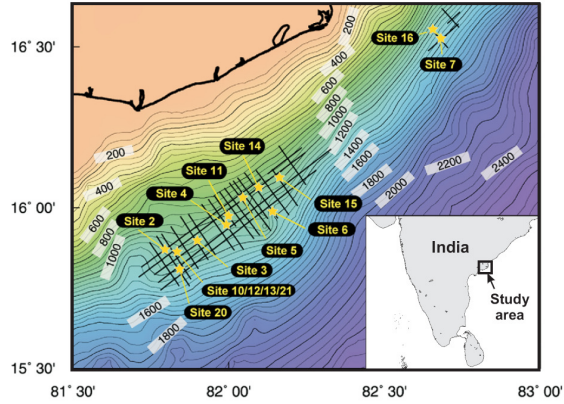


Figure 1: Location of different drilled sites of NGHP-01 in KG-basin (modified from Collett et al., 2008).

The Site NGHP-01-15 (Prospectus Site GDGH11) is located in the northern part of the Krishna-Godavari (KG) Basin (Figure 1). The site was selected as an alternate location in the program and was not part of the pre-coring logging-while-drilling/measurement-while-drilling (LWD/MWD) program. The water depth at this site is ~926 m. The seismic data from Site NGHP-01-15 show a typical KG Basin sequence of ridges and basins with a well developed BSR at depth of 126 mbsf. This site does not show the steeply-dipping, high-reflectivity layers below the BSR that characterizes other KG Basin sites drilled during this expedition; rather the sediments are more flat lying. The lithostratigraphy recovered at Site NGHP-01-15 is generally described as nanofossil bearing-clay; with relatively thick sand laminae and beds (of various thicknesses). Interstitial water analysis of cores from Hole NGHP-01-15A indicate the presence of localized beds containing concentrated gas-hydrates occurrence within the depth interval from about 60 to 90 mbsf. Gas-hydrates was observed and sampled from one core at depth of 78.63-79.13 mbsf in Hole NGHP-01-15A, which also exhibited a relatively continuous IR anomaly (~9 m in length) when imaged on the catwalk. Mousse sediment textures (formed during gas-hydrates dissociation) were also observed within the cores recovered from Hole NGHP-01-15A. Physical observations of the core on the catwalk, confirmed that the IR imaged and sampled gas-hydrates in the interval 78.63-79.13 mbsf occurred in a prominent sand bed. Gas-hydrates, associated with clean sand and woody debris, was also recovered in a pressure core from a depth of 86.7 mbsf

in Hole NGHP-01-15A. Relatively high resistivity values measured during the wireline logging program in Hole NGHP-01-15A above ~110 mbsf suggest that some gas-hydrates is present above this depth. The highest resistivity values between about 75 and 81 mbsf correspond to the section in which the strong temperature anomalies were measured on the catwalk and gas-hydrates samples were recovered.

Effective Medium Theory

The effective medium theory (EMT), a combination of self-consistent approximation (SCA) and differential effective medium (DEM) theory, was basically developed to determine the elastic properties of sedimentary rock (Sheng 1990, 1991) and shale (Hornby et al. 1994). The effective medium is created by implanting inclusions of one material within another material. Both SCA and DEM methods determine the effective elastic moduli of a medium from the individual components and their geometry. In marine sediments, grains and pore-fluids are fully connected (bi-connected medium) at all realistic porosities. But SCA and DEM individually can not model such medium which is bi-connected at all porosities. SCA constructs bi-connected medium within 40-60% porosity and it is not valid above 60% porosity (Sheng 1990, 1991; Hornby et al. 1994). DEM models micro-structure of a medium but it depends absolutely on the status of the starting medium. If the starting medium is biconnected which can be modeled by SCA within 40-60% porosity, then DEM determines the effective elastic properties preserving the bi-connectivity of the medium at all porosities. Jakobsen et al. (2000) extended the theory to determine the elastic property of gas hydrate-bearing sediment. According to this theory two end member distributions of gas hydrate are considered : (1) non-load bearing gas hydrate in which gas hydrate is a part of the pore fluid, and remains without appreciable grain contact (non-contact model) and (2) load-bearing gas hydrate where gas hydrate cements the grains and form a continuous matrix (contact model).

A large fraction of the offshore sedimentary basins are clay-rich and clay platelets in marine sediments commonly prefer horizontal alignments, which exhibit anisotropic elastic behavior in the long wavelength limits (Hornby et al. 1994; Sayers 1994; Chlach and Schmitt 2006). Clay platelets form the connected skeleton of the sediment and silt minerals remain as the isolated phase. Abundance of



phyllosilicate minerals such as clays in sediments contribute to the overall anisotropy of many rocks because of large anisotropy of the phyllosilicate single crystals and their texture, quantitatively described by an orientation distribution function (ODF) (Cholach and Schmitt 2006). Groups of clay-platelets (domains) are fully aligned locally, but the orientation of these groups of clay platelets may vary depending on the depositional and stress history of the sediment (Jakobsen et al. 2000; Hornby et al. 1994; Sayers 1994). The orientation of these crystalline aggregates varies from completely aligned (transversely isotropic) to completely disorder (isotropic). The degree of anisotropy depends on the precise orientation distribution pattern of the clay platelets. The average elastic properties of partially aligned clay platelets are computed by the method of smoothing (Bonilla and Keller 1985).

In modeling procedure, the starting phase for the non-load bearing model is composed of pore water and clay particles whose effective elastic moduli are calculated by the SCA-DEM method. Gas hydrate is then included by replacing water, leaving the clay concentration unchanged. Here, the effective microstructure is connected clay (load-bearing), connected water and unconnected gas hydrate (non-load-bearing). Gas hydrate has the same aspect ratio (1/20) and orientation as the clay platelets (Hornby et al. 1994; Jakobsen et al. 2000). After incorporating the anisotropy due to orientation distribution pattern of clay platelets, quartz is included in the aggregated clay-water-gas hydrate composite using the DEM method. The concentration of quartz is increased successively from zero to the desired volume replacing all other constituents in proportion to the volume fraction of the inclusion (quartz) and other constituents. A spherical inclusion model (aspect ratio of 1) is used for quartz (Hornby et al. 1994). Roles of water and gas hydrate are interchanged in the load-bearing model of gas hydrate.

Data

The sonic P- and S-wave velocities (Figure 2a) are obtained from processed Dipole Sonic Imager (DSI) Pass-I mode waveform (Collett et al., 2008).

The standard density log in Hole 15A, is used to calculate the sediment porosities (ϕ) with the standard density-porosity relation: $\phi = (\rho_g - \rho_b) / (\rho_g - \rho_w)$, shown in

Figure 2b. Here, water density (ρ_w) is taken as 1.03 g/cm³ and the grain density measured on core samples (Collett et al., 2008) by using at each depth the grain density from the closest sample. Hence the good agreement between the density-porosity log and the porosity measurements from core samples is a direct consequence of the good agreement in the density data. The mineralogical composition is taken from the smear slide analysis of Hole 15A, the variation of which with depth is shown in Figure 2c. Two resistivity measurements are used to derive the formation resistivity shown in Figure 2a. The Spherically Focused unaveraged resistivity (SFLU) has the highest resolution, but the shallowest penetration, of the resistivity measurements made by the DIT tool and is more sensitive to drilling disturbances; the Deep Induction Log (ILD) has the deepest penetration, but a lower vertical resolution. The combination of these two estimates provides a possible range of gas-hydrates distribution around Hole NGHP-01-15A. Elastic properties of the primary constituents of the sediment are given in Table 1.

Constituents	ρ (g/cm ³)	K (GPa)	μ (GPa)
Clay	2.60	21.2	6.66
Water	1.03	2.25	0
Hydrate	0.92	8.37	3.68
Quartz	2.70	37.79	44.07

Table 1: Densities (ρ), bulk moduli (K) and shear moduli (μ) of different constituents of the sediment [after Jakobsen et al., 2000] used for modeling. Density of water is taken from Collett et al. [2008b].

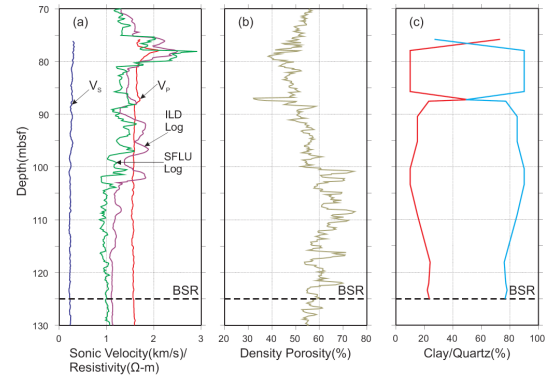


Figure 2: (a) Sonic P- and S-wave velocities, ILD and SFLU resistivity log (b) Density-porosity and (c) percentage of clay (red) and quartz (blue) at different depths.



Method

Determination of the ODF of clay platelets

Since, there is no published orientation distribution pattern of clay platelets in the KG basin; we determine the coefficients of ODF from other available data. In case of VTI medium, the ODF of clay-particle is a function of two coefficients W_{200} , which varies from 0 (completely disordered clay platelets) to 0.04005 (completely aligned clay platelets) and W_{400} , which varies from 0 (completely disordered clay platelets) to 0.05373 (completely aligned clay platelets) [Sayers, 1994]. These coefficients are determined by matching observed background P- and S-wave sonic velocities with theoretical velocities computed using the combined SCA/DEM theory by varying W_{200} and W_{400} from their minimum to maximum values (Figure 3). The crossing point of observed P- and S-wave velocities gives the values of W_{200} and W_{400} for the region concerned.

Quantification of gas-hydrates by EMT and other standard techniques

The amount of gas-hydrates at Site 15 is quantified by the EMT using the determined coefficients of the ODF. The gas hydrate saturation depth function is compared with other standard rock physics models like Biot-Gassman Theory modified by Lee (BGTL, Lee, 2002), EMT of Helgerud et al. (1999) and resistivity log using Archie's law (Archie, 1942). In resistivity method Archie's parameters are taken as $a = 1$, $m = 2.1$ and $n = 2$ (Collett et al., 2008).

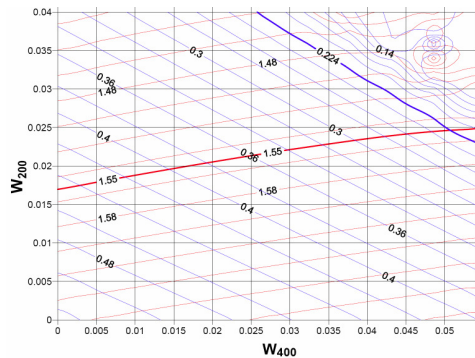


Figure 3: Computed P- (red) and S- (blue) wave velocities for various W_{200} and W_{400} . Thick red and blue lines are the background

sonic P- and S-wave velocities, intersection of which gives the coefficients of ODF for clay platelets.

Results

The distribution function of clay platelets is determined from background sonic P- (1.55 km/s) and S-wave (224 m/s) velocities at ~116 mbsf of no-gas hydrate/ no-free-gas sample from Hole NGHP-01-15A (Collett et al., 2008) in the KG basin. The sample is silty-clay with porosity of 63.5 %. Figure 3 shows the determined distribution coefficients for ODF which are $W_{400} = 0.0508$ and $W_{200} = 0.0248$.

Using this ODF, the background velocities are computed from the combined SCA/DEM method and other standard rock physics models (Figure 4a). Figure 4b shows the gas-hydrates saturation with depths using the SCA/DEM and comparison with other rock physics models. Maximum gas hydrate saturation from the EMT is estimated as ~50% at about 80 mbsf for non-contact distribution model of gas-hydrates.

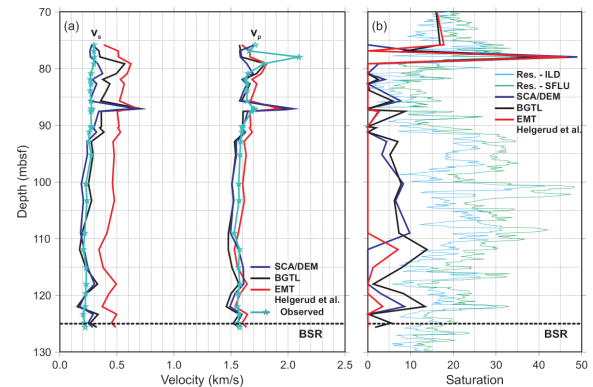


Figure 4: (a) Background velocities computed by different rock physics models and compared with the observed velocities, (b) Hydrate saturation with depth determined from different rock physics models and resistivity log.

Discussion and conclusions

The accuracy of the determined coefficients of orientation distribution function is verified by comparing the computed background velocities by the combined SCA/DEM theory with the observed velocities. It is obvious from Figure 4a, that the background velocities computed from the combined SCA/DEM theory fit best with the observed velocities. Figure 4b shows the saturation of gas-hydrates



with depth by different methods. The average saturation is higher (~25%) from both type of resistivity logs than the other rock physics models. Saturation from EMT of Helgerud et al. (1999) is minimum and approximately zero at most of the depths except ~46% at 77 mbsf. BGTL model shows higher value than the combined SCA/DEM model except at 77 mbsf where saturation determined from SCA/DEM is maximum ~49%. Contact distribution model of gas-hydrates in SCA/DEM method do not give any finite saturation value. Therefore, it is concluded that the gas-hydrates is distributed within the pore spaces without appreciable grain contact.

A better match between the computed background velocities from the combined SCA/DEM theory and the observed velocities than other rock physics models indicates a better prediction of gas-hydrates saturation by the SCA/DEM theory. Archie's law gives higher hydrate saturation, which may be due to the fact that the gas-hydrates acts as pore freshening and it increases the formation resistivity which in turn increases the hydrate saturation.

References

Archie, G. E., 1942, The electrical resistivity log as an aid in determining some reservoir characteristics; *J. Pet. Technol.*, 5, 1-8.

Bonilla, L. L. and Keller, J. B., 1985, Acoustoelastic effect and wave propagation in heterogeneous weakly anisotropic materials; *J. Mech. Phys. Solids*, 33, 241-261.

Cholach, P. Y. and Schmitt D. R., 2006, Intrinsic elasticity of a textured transversely isotropic muscovite aggregate: Comparisons to the seismic anisotropy of schists and shales; *J. Geophys. Res.*, 111, B09410.

Collett, T., Riedel, M., Cochran, J., Boswell, R., Presley, J., Kumar, P., Sathe, A., Sethi, A., Lall, M., Sibal, V. and the NGHP Expedition 01 Scientists, 2008, Indian National Gas hydrate Program Expedition 01 Initial Reports; DGH, India.

Helgerud, M. B., Dvorkin, J., Nur, A., Sakai, A. and Collett, T., 1999, Elastic-wave velocity in marine sediments with gas hydrates: effective medium modeling; *Geophys. Res. Lett.*, 26, 2021-2024.

Hornby, B. E., Schwartz, L.M. and Hudson, J. A., 1994, Anisotropic effective medium modeling of the elastic properties of shales, *Geophys.*, 59, 1570-1583.

Jakobsen, M., Hudson, J. A., Minshull, T. A. and Singh, S. C., 2000, Elastic properties of hydrate-bearing sediments using effective medium theory, *J. Geophys. Res.*, 105, 561-577.

Lee, M.W., 2002, Biot-Gassmann theory for velocities of gas hydrate bearing sediments; *Geophysics*, 67, 1711-1719.

Sayers, C. M., 1994, The elastic anisotropy of shales; *J. Geophys. Res.*, 99, 767-774.

Sheng, P., 1990, Effective medium theory of sedimentary rocks; *Physical Review*, B 41, 4507-4512.

Sheng, P., 1991, Consistent modeling of the electrical and elastic properties of sedimentary rocks; *Geophys.*, 56(8), 1236-1243.

Acknowledgments

We are grateful to the Director, NGRI for his kind consent to publish this work. We thank the Directorate General of Hydrocarbons, India and the NGHP Expedition-01 Scientific Party for collecting and providing the valuable data